Journal of Interconnection Networks
Vol. 14, No. 1 (2013) 1350002 (24 pages)

DOI: 10.1142/S0219265913500023

World Scientific
www.worldscientific.com

DIMENSION-ORDER ROUTING ALGORITHMS FOR A FAMILY OF MINIMAL-DIAMETER CIRCULANTS

PRANAVA K. JHA
Department of Computer Science
St. Cloud State University
720 Fourth Ave. S.
St. Cloud, MN 56301-4498, USA
pkjha@stcloudstate.edu

Received 29 March 2013
Revised 16 May 2013

This paper presents a family of minimal-diameter, four-regular nonbipartite circulants on $2a^2$ vertices, where a is odd. If $a \equiv 3 \bmod (4)$, then the step sizes are 1 and $(a-1)^2$, and if $a \equiv 1 \bmod (4)$, then the step sizes are 1 and $(a+1)^2$. Each graph is obtainable from the $2a \times a$ rectangular twisted torus by appropriately trading a total of $3a-1$ edges for as many new edges. Further, each admits an almost-square L-shaped embedding in the two-dimensional Cartesian plane, facilitating a plane tessellation that leads to an efficient dimension-order routing algorithm.

Keywords: Graphs and networks; circulant graphs; rectangular twisted torus; dimension-order routing algorithms; network topology; processor interconnection.

1. Introduction

The *circulant graphs* constitute a subfamily of Cayley graphs.[12] They find applications in areas such as distributed systems, VLSI and parallel machines.[3,5,13,19] Some of their welcome features include high symmetry, Hamiltonian decomposability and a high degree of fault tolerance. Accordingly, they have been a topic of deep studies for long.[2,4,18]

Routing is the process of selecting paths in a *graph/network* along which to send the traffic.[9] It is a vital component of all active networks. Unfortunately, the related problem of tracing a shortest path in a circulant is NP-hard.[6] Nevertheless it is possible to build families of circulants that are diameter-optimal. See Refs. [10] and [11] for efficient routing in circulants.

We build the following circulants from the $2a \times a$ *rectangular twisted torus* (RTT)[7] by trading a total of $3a-1$ edges for as many new edges: (i) $\mathcal{C}_{2a^2}(1, (a-1)^2)$, $a \equiv 3 \pmod 4$, and (ii) $\mathcal{C}_{2a^2}(1, (a+1)^2)$, $a \equiv 1 \pmod 4$. Further, we present *dimension-order routing algorithms* for them.

1.1. *Motivation*

The circulants in the present study constitute a new family. They are derived from the RTT, which lends them the advantages of the diameter being minimal, and the average distance being equal to two-thirds of the diameter. (There is no known formula for the diameter of a circulant.)

The circulants themselves turn out to be nonbipartite, and their odd girth (i.e., the length of a shortest odd cycle) is equal to $\sqrt{2n} - 1$, where n is the order of the graph. (A high odd girth is a plus in a network.) Further, the routing schemes we build are amenable to an easy implementation.

1.2. *Dimension-order routing*

The dimension-order routing relies on embedding the network in the Cartesian plane, where the shortest distance between a source and the destination is equal to the sum of the offsets in the orthogonal dimensions.[9] A packet is routed by progressively "reducing" the offset in one dimension to zero before considering the offset in the other dimension. Advantages include ease of implementation and deadlock avoidance between dimensions.

Toward a dimension-order routing, we construct a 2D representation of the circulant leading to a plane tessellation.[20] This approach has been utilized in several studies.[7,8,16]

1.3. *Definitions and preliminaries*

When we speak of a graph G, we mean a finite, simple, undirected and connected graph. Let $dia(G)$ represent the diameter of G. Vertices that are at a distance of $dia(G)$ from a vertex, say u, are called *diametrical* relative to u. We employ *vertex* and *node* as synonyms. For missing details, see Ref. [9].

Let C_n denote a *cycle* on n vertices, where $n \geq 3$, and where adjacencies exist in the natural way. The *Cartesian product* $G\Box H$ of graphs $G = (V, E)$ and $H = (W, F)$ is defined as follows: $V(G\Box H) = V \times W$ and $E(G\Box H) = \{\{(a, x), (b, y)\}: \{a, b\} \in E$ and $x = y$, or $\{x, y\} \in F$ and $a = b\}$. The graph $C_m\Box C_n$ is also known as the $m \times n$ *torus*.

Let n, r and s be positive integers, where $n \geq 6$, and $1 \leq r < s < n/2$. A four-regular circulant $\mathcal{C}_n(r, s)$ has $\{0, \cdots, n-1\}$ as its vertex set and $\{\{i,\ i \pm r\}$, $\{i,\ i \pm s\} : 0 \leq i \leq n-1\}$ as its edge set, where $i \pm r$ and $i \pm s$ are each modulo n. Fig. 1 presents $\mathcal{C}_{18}(1,\ 4)$ and its (distance-wise) level diagram, where vertices diametrical relative to 0 appear within "rectangles."

1.4. *Rectangular twisted torus (RTT)*

The $2a \times a$ rectangular twisted torus (RTT)[7] is an alternative to the $2a \times a$ torus. Its vertex set is given by $\{(i,\ j) : 0 \leq i \leq 2a - 1$ and $0 \leq j \leq a - 1\}$, while its edge set consists of the following:

- $\{(i,j),(i+1,j)\}$: $0 \le i \le 2a-2$ and $0 \le j \le a-1$ ("horizontal" edges)
- $\{(i,j),(i,j+1)\}$: $0 \le i \le 2a-1$ and $0 \le j \le a-2$, ("vertical" edges)
- $\{(0,j),(2a-1,j)\}$: $0 \le j \le a-1$, ("wrap-around" edges), and
- $\{(i,0),(i+a,a-1)\}$: $0 \le i \le 2a-1$, ("twisted" edges).

The arithmetic is modulo $2a$ (resp. a) in the first (resp. second) co-ordinate.

The RTT is four-regular, bipartite and Hamiltonian decomposable.[14] Its distance-wise vertex distribution[7] is given by $1+\underbrace{4i}_{1\le i\le a-1}+(2a-1)$. Fig. 2 (analogous to Fig. 1) presents the 6×3 RTT and its level diagram.

1.5. *State of the art*

The circulants enjoy a rich literature. See Ref. [1] and Ref. [4] that deal with their isomorphism and connectivity, respectively.

Toward finding a shortest path in a circulant, Wong and Coppersmith[20] presented a geometrical approach that has since proved to be very useful. See Ref. [21] and the surveys[3,13] for related issues.

Among various circulants, those of degree four are especially useful. Issues relating to their interconnection schemes, optimal layouts and isomorphism have been examined at length.[2,15,17] See Ref. [18] for recent results.

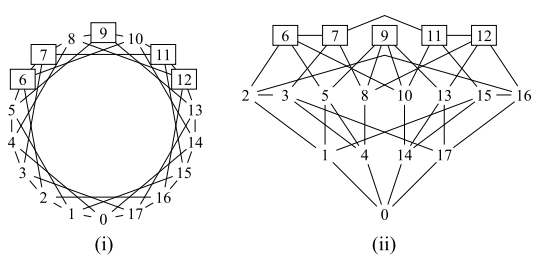

Fig. 1. The circulant $\mathcal{C}_{18}(1, 4)$ and its level diagram.

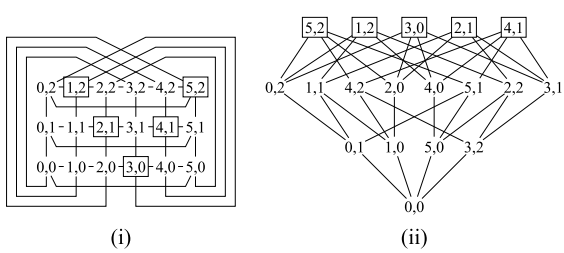

Fig. 2. 6×3 RTT and its level diagram.

1.6. *What follows*

- Sec. 2: $\mathcal{C}_{2a^2}(1,(a-1)^2)$, $a \equiv 3 \pmod 4$
  - (a) A mapping from the vertex set of the RTT to that of the circulant, and the inverse of the mapping showing that it is a bijection.
  - (b) Transformation of the RTT into the circulant through a trade of $3a-1$ edges for as many new edges.
- Sec. 3: $\mathcal{C}_{2a^2}(1,(a+1)^2)$, $a \equiv 1 \pmod 4$: Analogous to Sec. 2.
- Sec. 4: Routing Algorithms
  - (a) Sec. 4.1: $\mathcal{C}_{2a^2}(1,(a-1)^2)$, $a \equiv 3 \pmod 4$: 2D representation, plane tessellation and routing scheme.
  - (b) Sec. 4.2: $\mathcal{C}_{2a^2}(1,(a+1)^2)$, $a \equiv 1 \pmod 4$: Analogous to Sec. 4.1.
- Sec. 5: Certain concluding remarks.

It is easy to see that $\mathcal{C}_{18}(1,2^2)$ and $\mathcal{C}_{50}(1,6^2)$ are optimal. In the remainder, let a be odd and greater than or equal to 7.

2. $\mathcal{C}_{2a^2}(1,(a-1)^2)$, $a \equiv 3 \pmod 4$

Table 1. Nomenclature in respect of Sec. 2, $a \equiv 3 \pmod 4$.

a:	parameter of the $2a \times a$ rectangular twisted torus (RTT) and the circulant $\mathcal{C}_{2a^2}(1,(a-1)^2)$
n:	number of vertices in the RTT/circulant, $n = 2a^2$
s:	parameter of the circulant, $s = (a-1)^2$, hence $n - s = a^2 + 2a - 1$
f:	mapping from the vertex set $\{0,\cdots,2a-1\} \times \{0,\cdots,a-1\}$ of the RTT to the vertex set $\{0,\cdots,2a^2-1\}$ of $\mathcal{C}_{2a^2}(1,(a-1)^2)$
S_i:	ordered sets in the partition of $\{0,\cdots,2a^2-1\}$, $0 \le i \le a$

See Table 1 for a set of terms that will be frequently used in the present section. The mapping f is given by

$$f(i,j) = \begin{cases} i + (n-s)j & i + j \le a-1, \text{ or } i+j = a \text{ and } i < j \\ i + (n-s)j + a^2 & i + j = a \text{ and } i > j, \text{ or} \\ & i + j \ge a+1 \text{ and } |i-j| \le a \\ i + (n-s)j - 2a & i - j \ge a+1 \end{cases} \tag{2.1}$$

the arithmetic being modulo n. (If $i + j = a$, then i and j cannot be equal, since a is odd.) The mapping is clearly well-defined. Fig. 3 illustrates it in respect of the 14×7 RTT, where (i,j) and $f(i,j)$ coexist at each node. Regions A, B and C correspond to the three cases, respectively, in Eq. (2.1). Nodes within rectangles are diametrical with respect to $(0,0)$ in the RTT. (The relevance of the "dark red" edges in the figure will be clear shortly.) Meanwhile Fig. 4 presents a general framework of vertex mapping in the light of Eq. (2.1), and Table 2 presents the regionwise node distribution in the RTT.

2.1. *f is a bijection*

For each i, $0 \le i \le a-2$, vertices in Region B on the ith row, followed by those in Region C on the $(i+1)$th row, and finally followed by those in Region A on that

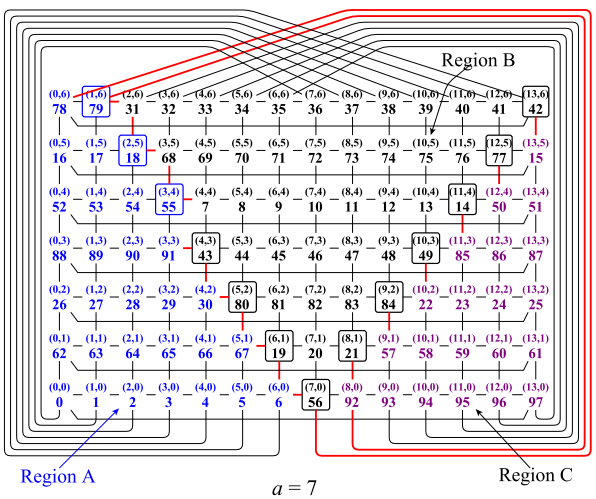

Fig. 3. 14×7 RTT in the light of Eq. (2.1).

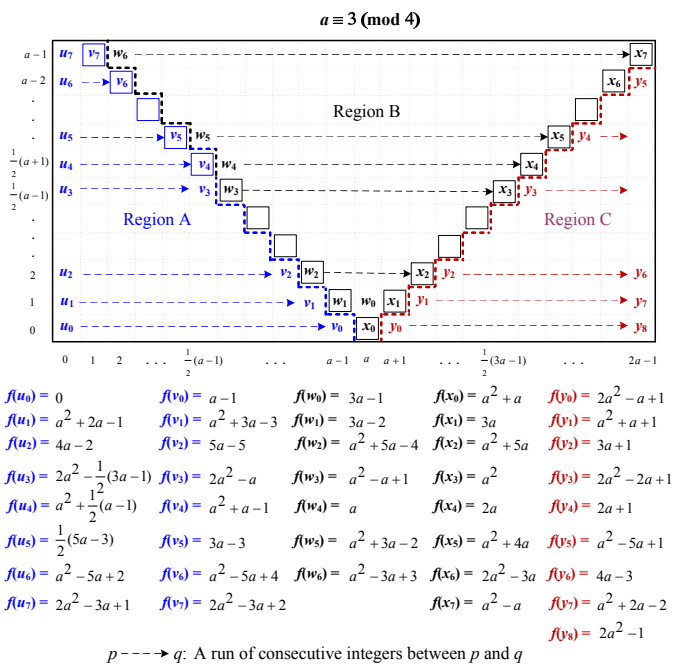

$f(u_0) = 0$ $f(v_0) = a-1$ $f(w_0) = 3a-1$ $f(x_0) = a^2+a$ $f(y_0) = 2a^2-a+1$

$f(u_1) = a^2+2a-1$ $f(v_1) = a^2+3a-3$ $f(w_1) = 3a-2$ $f(x_1) = 3a$ $f(y_1) = a^2+a+1$

$f(u_2) = 4a-2$ $f(v_2) = 5a-5$ $f(w_2) = a^2+5a-4$ $f(x_2) = a^2+5a$ $f(y_2) = 3a+1$

$f(u_3) = 2a^2-\frac{1}{2}(3a-1)$ $f(v_3) = 2a^2-a$ $f(w_3) = a^2-a+1$ $f(x_3) = a^2$ $f(y_3) = 2a^2-2a+1$

$f(u_4) = a^2+\frac{1}{2}(a-1)$ $f(v_4) = a^2+a-1$ $f(w_4) = a$ $f(x_4) = 2a$ $f(y_4) = 2a+1$

$f(u_5) = \frac{1}{2}(5a-3)$ $f(v_5) = 3a-3$ $f(w_5) = a^2+3a-2$ $f(x_5) = a^2+4a$ $f(y_5) = a^2-5a+1$

$f(u_6) = a^2-5a+2$ $f(v_6) = a^2-5a+4$ $f(w_6) = a^2-3a+3$ $f(x_6) = 2a^2-3a$ $f(y_6) = 4a-3$

$f(u_7) = 2a^2-3a+1$ $f(v_7) = 2a^2-3a+2$ $f(x_7) = a^2-a$ $f(y_7) = a^2+2a-2$

$f(y_8) = 2a^2-1$

Fig. 4. Vertex labeling of the RTT in the light of Eq. (2.1).

Table 2. Regionwise distribution of vertices in the RTT (cf. Fig. 4).

Region	Row i contains nodes $\cdots$	$-i-$	no. of nodes
A	$(0,i)$ to $(a-i-1,i)$	0 to $\frac{1}{2}(a-1)$	$a-i$
	$(0,i)$ to $(a-i,i)$	$\frac{1}{2}(a+1)$ to $a-1$	$a-i+1$
B	$(a-i,i)$ to $(a+i,i)$	0 to $\frac{1}{2}(a-1)$	$2i+1$
	$(a-i+1,i)$ to $(a+i,i)$	$\frac{1}{2}(a+1)$ to $a-1$	$2i$
C	$(a+i+1,i)$ to $(2a-1,i)$	0 to $a-2$	$a-1-i$

There is no vertex on the $(a-1)$th row in Region C.

row receive labels that constitute an unbroken sequence (modulo n) of integers. In that light, the set $\{0,\cdots,2a^2-1\}$ admits a partition into ordered sets $S_0,\cdots,S_a$. (See Table 3.) Whereas $S_{\frac{1}{2}(a-1)}$ and S_a are each of size $2a-1$, the remaining are of size $2a-2$ each. See Fig. 5 for the partition for $a=7$.

Table 3. Partition of $\{0,\cdots,2a^2-1\}$ into sets $S_0,\cdots,S_a$, $a\equiv 3 \pmod 4$.

S_i	$\lvert S_i\rvert$	
$\{2(a-1)i+a,\cdots,2(a-1)i+3(a-1)\}$	$2a-2$	$0\le i\le \frac{1}{2}(a-3)$
$\{2(a-1)i+a,\cdots,2(a-1)i+3a-2\}$	$2a-1$	$i=\frac{1}{2}(a-1)$
$\{2(a-1)i+a+1,\cdots,2(a-1)i+3a-2\}$	$2a-2$	$\frac{1}{2}(a+1)\le i\le a-1$
$\{2a^2-a+1,\cdots,2a^2-1\}\cup\{0,\cdots,a-1\}$	$2a-1$	$i=a$

Lemma 2.1. *The following identities hold:*

(i) $f(a+i+1,i)=1+f(a+i-1,i-1)$, $0\le i\le a-2$.
(ii) $f(0,i)=1+f(2a-1,i)$, $0\le i\le a-2$.

Proof. For (i), note that $(a+i+1,i)$ is in Region C, and $(a+i-1,i-1)$ is in Region B. Accordingly, $f(a+i+1,i)=\big(a+i+1+(a^2+2a-1)i-2a\big) \bmod 2a^2$ that is $\big(1+a^2i+(2i-1)a\big) \bmod 2a^2$, and $f(a+i-1,i-1)=\big(a+i-1+(a^2+2a-1)(i-1)+a^2\big) \bmod 2a^2$ that is $\big(a^2i+(2i-1)a\big) \bmod 2a^2$. It is clear that $(1+a^2i+(2i-1)a)$ cannot be a multiple of $2a^2$, hence $f(a+i+1,i)=1+f(a+i-1,i-1)$.

For (ii), note that $(0,i)$ is in Region A, and $(2a-1,i)$ is in Region C. Accordingly, $f(0,i)=\big((a^2+2a-1)i\big) \bmod 2a^2$ that is $\big(a^2i+2ai-i\big) \bmod 2a^2$, and $f(2a-1,i)=\big(2a-1+(a^2+2a-1)i-2a\big) \bmod 2a^2$ that is $\big(a^2i+2ai-i-1\big) \bmod 2a^2$. Since a is odd and $0\le i\le a-2$, it is clear that $(a^2i+2ai-i)$ cannot be a multiple of $2a^2$, hence $f(0,i)=1+f(2a-1,i)$. □

Lemma 2.2. *The function f in Eq. (2.1) is a bijection.*

Proof. Let T_i denote the set of vertices of the RTT such that $(u, v) \in T_i \Leftrightarrow f(u, v) \in S_i$, $0 \leq i \leq a$. (Labels to vertices in the same row within a particular region constitute a run of integers.) The following are in order:

(i) For $0 \leq i \leq \frac{1}{2}(a-1)$, the smallest element $2(a-1)i + a$ of S_i is equal to $f(a-i, i)$ if i is odd, and $f(\frac{1}{2}(a+1) - i, i + \frac{1}{2}(a+1))$ if i is even.
   (a) i odd: T_i consists of $(a-i, i), \cdots, (a+i, i)$ from Region B, $(a+i+2, i+1), \cdots, (2a-1, i+1)$ from Region C, and $(0, i+1), \cdots, (a-i-2, i+1)$ from Region A. (For $i = \frac{1}{2}(a-1)$, the sequence goes up to $(a-i-1, i+1)$.)
   (b) i even: T_i consists of $(\frac{1}{2}(a+1)-i, i+\frac{1}{2}(a+1)), \cdots, (i+\frac{1}{2}(3a+1), i+\frac{1}{2}(a+1))$ from Region B, $(i+\frac{1}{2}(3a+5), i+\frac{1}{2}(a+3)), \cdots, (2a-1, i+\frac{1}{2}(a+3))$ from Region C, and $(0, i+\frac{1}{2}(a+3)), \cdots, (\frac{1}{2}(a+3)-i, i+\frac{1}{2}(a+3))$ from Region A.

(ii) For $\frac{1}{2}(a+1) \leq i \leq a-1$, the smallest element $2(a-1)i + a + 1$ of S_i is equal to $f(a+1-i, i)$ if i is odd, and $f(\frac{1}{2}(3a+1) - i, i - \frac{1}{2}(a+1))$ if i is even.
   (a) i odd: T_i consists of $(a+1-i, i), \cdots, (a+i, i)$ from Region B, $(a+i+2, i+1), \cdots, (2a-1, i+1)$ from Region C, and $(0, i+1), \cdots, (a-1-i, i+1)$ from Region A. (Region C being null on the $(a-1)$th row, T_{a-2} has no vertex from C.)
   (b) i even: T_i consists of $(\frac{1}{2}(3a+1)-i, i-\frac{1}{2}(a+1)), \cdots, (i+\frac{1}{2}(a-1), i-\frac{1}{2}(a+1))$ from Region B, $(i+\frac{1}{2}(a+3), i-\frac{1}{2}(a-1)), \cdots, (2a-1, i-\frac{1}{2}(a-1))$ from Region C, and $(0, i-\frac{1}{2}(a-1)), \cdots, (\frac{1}{2}(3a-3)-i, i-\frac{1}{2}(a-1))$ from Region A.

(iii) $T_a = \{(a+1, 0), \cdots, (2a-1, 0), (0, 0), \cdots, (a-1, 0)\}$.

It follows that there exists a one-to-one correspondence between each S_i and T_i. To conclude the proof, note that the last element (p, q) of T_i and the first element (u, v) of T_{i+1} are such that $f(u, v) = 1 + f(p, q)$, $0 \leq i \leq a-1$. □

Fig. 5 illustrates the proof of Lemma 2.2. The colors assigned to various nodes are same as those in Fig. 3.

2.2. *Transforming the RTT into* $C_{2a^2}(1, (a-1)^2)$

Call an edge $\{(i, j), (p, q)\}$ in the RTT *incompatible* if $|f(p, q) - f(i, j)| \bmod n$ is different from each of 1, $n-1$, s and $n-s$, and call it *compatible* otherwise.

Lemma 2.3. *Except for the edges appearing in Fig. 6(i), each edge in the RTT is compatible.*

Note: There are $3a-1$ incompatible edges in Fig. 6(i). They appear as dark red lines in Fig. 3. Each is incident to a diametrical vertex, and not more than two are incident to any diametrical vertex.

Proof. (Lemma (2.3)

- Horizontal edges: The horizontal edges within a particular region are necessarily compatible. Here are those running across Region B and Region C: $\{(a+i,i),(a+i+1,i)\}$, $0 \leq i \leq 1-2$. Check to see that $|f(a+i,i) - f(a+i+1,i)| \bmod n$ is equal to s or $n-s$. (See Figs. 3 and 4.) The remaining horizontal edges run across Region A and Region B, and they are forbidden.
- Wrap-around edges: It is easy to see that $f(0,i) = 1 + f(2a-1,i) \bmod n$, $0 \leq i \leq a-2$, and $f(0,a-1) = s + f(2a-1,a-1)$.
- Vertical edges: For $\{(i,j),(i,j+1)\}$ within a particular region, $|f(i,j) - f(i,j+1)| \bmod n$ equals s or $n-s$. Those remaining are forbidden.
- Twisted edges: For $0 \leq i \leq a-1$, $(i,0)$ is in Region A while $(i+a,a-1)$ is in Region B. Check to see that $f(i+a,a-1) = f(i,0)+(a-1)^2$, hence the edges $\{(i,0),(i+a,a-1)\}$ are compatible. For $2 \leq i \leq a-1$, $(i,a-1)$ is in Region B while $(i+a,0)$ is in Region C, and $f(i,a-1) = f(i+a,0)+(a-1)^2$, hence the edges $\{(i,a-1),(i+a,0)\}$ are compatible. The rest i.e., $\{(a,0),(0,a-1)\}$ and $\{(a+1,0),(1,a-1)\}$ are forbidden. □

Lemma 2.4. *The graph obtainable from the $2a \times a$ RTT by replacing the edges from Fig. 6(i) by those from Fig. 6(ii) is isomorphic to $\mathcal{C}_{2a^2}(1,(a-1)^2)$.*

Proof. The edges in Fig. 6(ii) are new in respect of the RTT, and the set of underlying vertices coincides with that in Fig. 6(i). Further, there are as many new edges as the incompatible edges, so it suffices to show that each new edge is compatible.

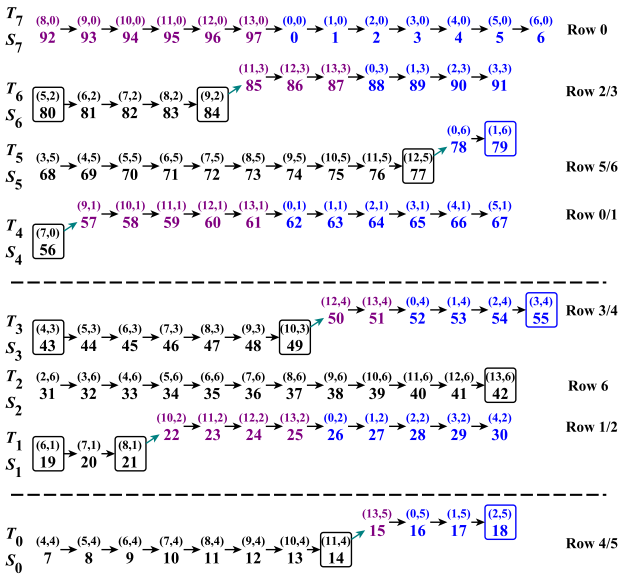

Fig. 5. Sets S_i and T_i in respect of the 14×7 RTT.

The new edges themselves are as follows:

- The a edges at the ath level (colored "green") in the form of a path of length a starting at $(a, 0)$ and ending at $(2a-1, a-1)$
- The $a-1$ edges in the form of a matching between the ath level and the $(a-1)$th level (colored "brown"), and
- The a edges at the $(a-1)$th level (colored "pink") in the form of a path of length a starting at $\left(\frac{1}{2}(a-1), \frac{1}{2}(a-1)\right)$ and ending at $\left(\frac{1}{2}(a+1), \frac{1}{2}(a+1)\right)$.

It is easy to check that each new edge is compatible. □

Note that the distance-wise node distribution of the RTT holds for the circulant as well, so the diameter of the circulant is equal to that of the RTT, i.e., a. See Fig. 7 for $\mathcal{C}_{98}(1, 36)$. The edge colors are as in Fig. 6(ii).

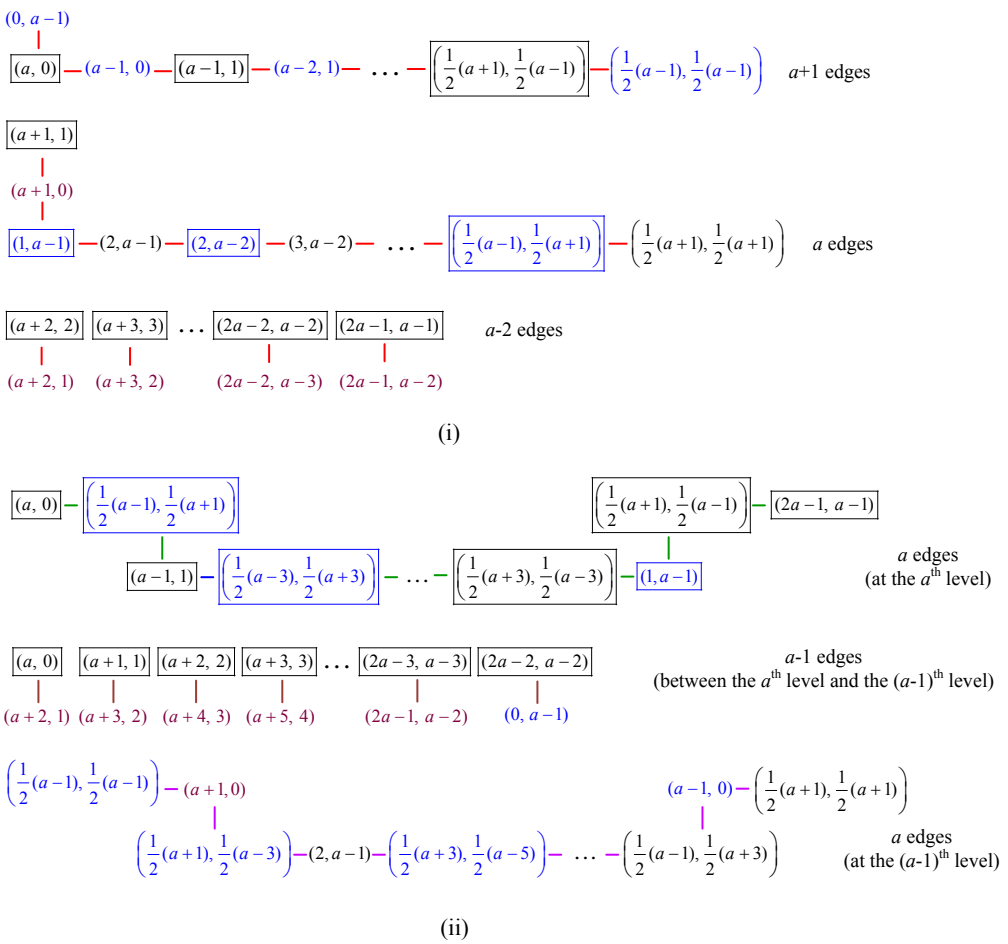

Fig. 6. (i) Incompatible edges in the RTT and (ii) New edges.

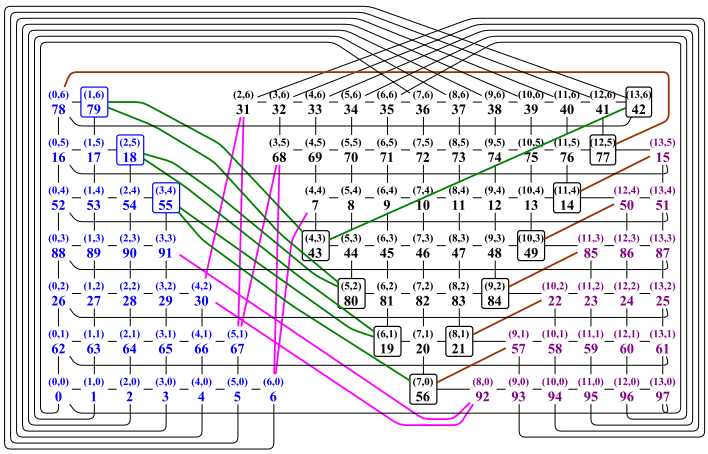

Fig. 7. $\mathcal{C}_{98}(1, 36)$ obtainable from the 14×7 RTT.

Table 4. Nomenclature in respect of Sec. 3, $a \equiv 1 \pmod 4$.

a:	parameter of the $2a \times a$ rectangular twisted torus (RTT) and the circulant $\mathcal{C}_{2a^2}(1, (a+1)^2)$
n:	number of vertices in the RTT/circulant, $n = 2a^2$
s:	parameter of the circulant, $s = n - (a+1)^2$, hence $n - s = (a+1)^2$
g:	mapping from the vertex set $\{0, \cdots, 2a-1\} \times \{0, \cdots, a-1\}$ of the RTT to the vertex set $\{0, \cdots, 2a^2-1\}$ of $\mathcal{C}_{2a^2}(1, (a+1)^2)$
S_i:	ordered sets in the partition of $\{0, \cdots, 2a^2-1\}$, $0 \le i \le a-1$

3. $\mathcal{C}_{2a^2}(1, (a+1)^2)$, $a \equiv 1 \pmod 4$

See Table 4 (that is analogous to Table 1 in Sec. 2) for a set of important terms in the present section. The mapping g is given by

$$g(i,j) = \begin{cases} i + (n-s)j & i + j \le a \\ i + (n-s)j + a^2 - 2a & i + j \ge a+1 \text{ and } |i-j| \le a-1, \text{or} \\ & i - j = a \text{ and } \frac{3a+1}{2} \le i \le 2a-1 \\ i + (n-s)j - 2a & i - j = a \text{ and } a+1 \le i \le \frac{3a-1}{2}, \text{or} \\ & i - j \ge a+1 \end{cases} \tag{3.1}$$

the arithmetic being modulo n. Meanwhile the schemes in this section are similar to those in Sec. 2, so routine details will be trimmed.

Fig. 8 illustrates the mapping in respect of the 18×9 RTT, and Fig. 9 presents a general framework of the vertex mapping in the light of Eq. (3.1). Further, Table 5 presents the regionwise node distribution in the RTT.

Table 5. Regionwise distribution of vertices in the RTT (cf. Eq. (3.1)).

Region	Row i contains nodes $\cdots$	$-i-$	no. of nodes
A	$(0,i)$ to $(a-i,i)$	0 to $a-1$	$a-i+1$
B	$(a-i+1,i)$ to $(a+i-1,i)$	1 to $\frac{1}{2}(a-1)$	$2i-1$
	$(a-i+1,i)$ to $(a+i,i)$	$\frac{1}{2}(a+1)$ to $a-1$	$2i$
C	$(a+1,0)$ to $(2a-1,0)$	0	$a-1$
	$(a+i,i)$ to $(2a-1,i)$	1 to $\frac{1}{2}(a-1)$	$a-i$
	$(a+i+1,i)$ to $(2a-1,i)$	$\frac{1}{2}(a+1)$ to $a-2$	$a-1-i$

There is no vertex on the 0th row in Region B.
There is no vertex on the $(a-1)$th row in Region C.

3.1. *g is a bijection*

Analogous to Table 3 in Sec. 2, Table 6 presents a partition of $\{0,\cdots,2a^2-1\}$ into ordered sets $S_0,\cdots,S_{a-1}$. Whereas S_0 is of size $2a$, half of the remaining sets are of size a each, and the rest are of size $3a$ each. Note that the smallest element u and the largest element v of each S_i are such that $u \equiv 1 \pmod{a}$ and $v \equiv 0 \pmod{a}$. For $a = 9$, the sets in the partition appear in Fig. 10.

Here is the analogue of Lemma 2.1.

Lemma 3.1. *The following identities hold:*

(i) $g(\frac{1}{2}(3a+1)+i, \frac{1}{2}(a-1)+i) = 1 + g(a-1+i,i)$, $1 \le i \le \frac{1}{2}(a-3)$.
(ii) $g(0,a-1) = 1 + g(\frac{3}{2}(a-1), \frac{1}{2}(a-1))$.

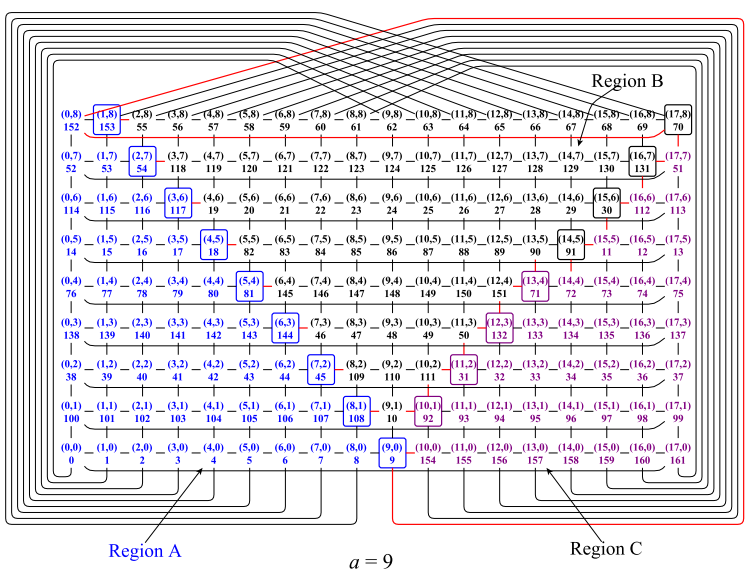

Fig. 8. 18×9 RTT in the light of Eq. (3.1).

Table 6. Partition of $\{0, \cdots, 2a^2-1\}$ into sets $S_0, \cdots, S_{a-1}$, $a \equiv 1 \pmod 4$.

S_i	$\lvert S_i \rvert$	
$\{n-a+1, \cdots, n-1, 0, \cdots, a\}$	$2a$	$i = 0$
$\{(2i-1)a+1, \cdots, 2ia\}$	a	i odd and $1 \le i \le \frac{1}{2}(a-1)$
$\{(2i-2)a+1, \cdots, (2i+1)a\}$	$3a$	i even and $2 \le i \le \frac{1}{2}(a-1)$
$\{(2i-1)a+1, \cdots, (2i+2)a\}$	$3a$	i odd and $\frac{1}{2}(a+1) \le i \le a-1$
$\{2ia+1, \cdots, (2i+1)a\}$	a	i even and $\frac{1}{2}(a+3) \le i \le a-1$

(iii) $g(a+i, i) = 1 + g(\frac{1}{2}(3a-1)+i, \frac{1}{2}(a-1)+i)$, $1 \le i \le \frac{1}{2}(a-1)$.

Proof. For (i), note that $(\frac{1}{2}(3a+1)+i, \frac{1}{2}(a-1)+i)$ is in Region C and $(a-1+i, i)$ is in Region B. Accordingly, $g(\frac{1}{2}(3a+1)+i, \frac{1}{2}(a-1)+i) = \big(\frac{1}{2}(3a+1)+i+(a+1)^2(\frac{1}{2}(a-1)+i)-2a\big) \bmod 2a^2$ that is $((i+1)a^2+(2i-1)a+2i) \bmod 2a^2$. Further, $g(a-1+i, i) = \big(a-1+i+(a+1)^2 i+a^2-2a\big) \bmod 2a^2$ that is $((i+1)a^2+(2i-1)a+2i-1) \bmod 2a^2$. Since $2 \le 2i \le (a-3)$, it is clear that $((i+1)a^2+(2i-1)a+2i)$ is not a multiple of $2a^2$. The claim follows. (ii) and (iii) are similar. □

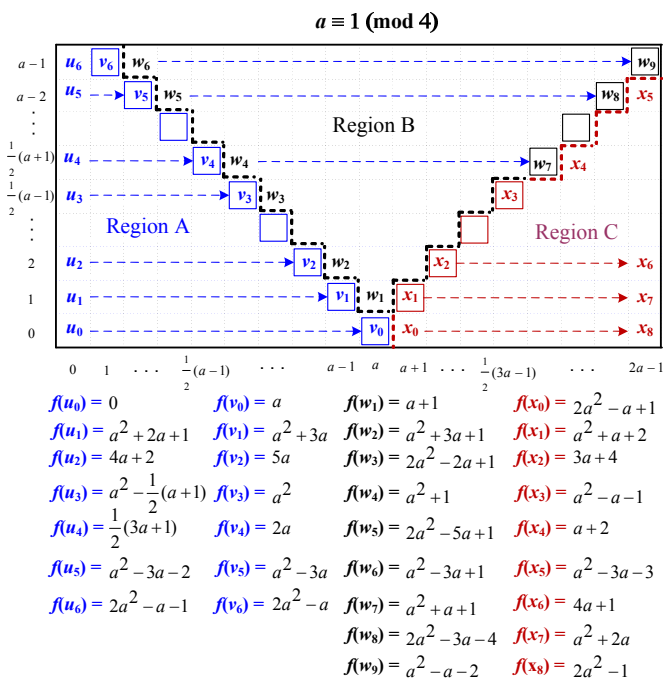

Fig. 9. Vertex labeling of the RTT in the light of Eq. (3.1).

Lemma 3.2. *The function g in Eq. (3.1) is a bijection.*

Proof. Let T_i be such that $(u, v) \in T_i \Leftrightarrow f(u, v) \in S_i$, $0 \leq i \leq a - 1$. It turns out that there exists a one-to-one correspondence between each S_i and T_i, and that $T_0, \cdots, T_{a-1}$ are mutually exclusive and exhaustive with respect to the vertex set of the RTT. Details are left to the reader. □

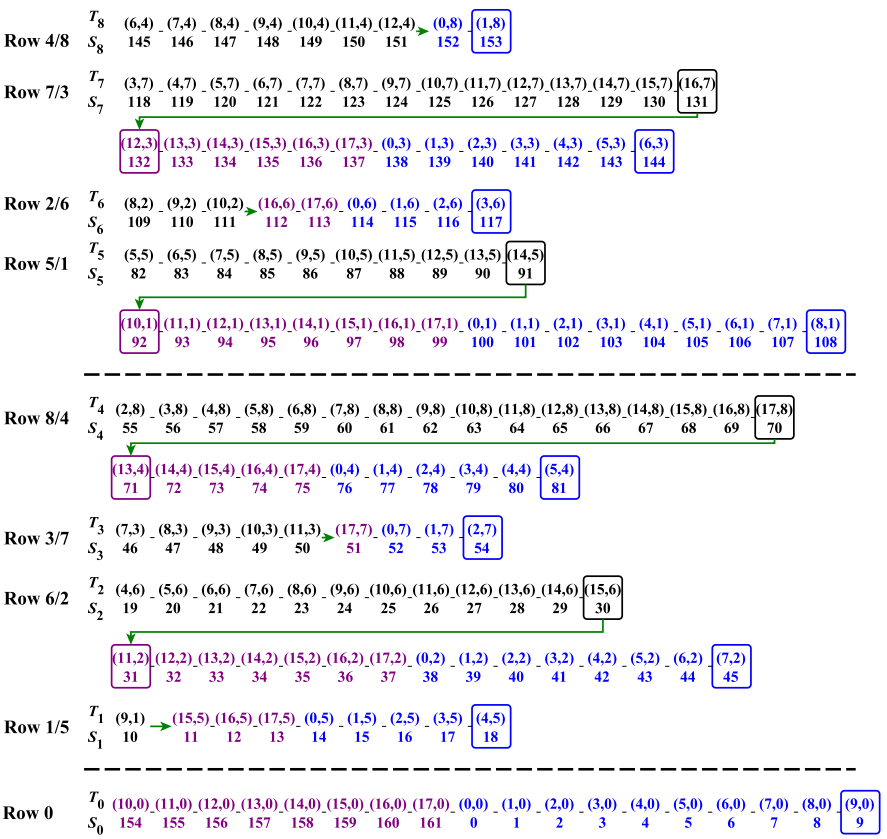

Fig. 10. Sets S_i and T_i in respect of the 18×9 RTT.

3.2. *Transforming the RTT into* $C_{2a^2}(1, (a+1)^2)$

Call an edge of the RTT (in)compatible as in Sec. 2.2.

Lemma 3.3. *Except for the edges appearing in Fig. 11(i), each edge in the RTT is compatible.*

Note: The number of incompatible edges is equal to $3a - 1$. Such edges appear as dark red lines in Fig. 8 in respect of the 18×9 RTT. It turns out that they exist

between the $(a-1)$th level and the ath level in the level diagram of the RTT, and their removal does not affect the connectedness.

Proof. (Lemma 3.3) Similar to the proof of Lemma 2.3. □

Lemma 3.4. *The graph obtainable from the $2a \times a$ RTT by replacing the edges from Fig. 11(i) by those from Fig. 11(ii) is isomorphic to $\mathcal{C}_{2a^2}(1, (a+1)^2)$.*

Proof. It suffices to show that each new edge is compatible. For convenience, the new edges are viewed to be of three types colored "green," "brown" and "pink," respectively, as shown in Fig. 11(ii). The rest of the argument is similar to that in the proof of Lemma 2.4. □

Based on a discussion as in Sec. 2, $dia(\mathcal{C}_{2a^2}(1, (a+1)^2)) = a$. Meanwhile Fig. 12 depicts $\mathcal{C}_{162}(1, 100)$. The color assignments are as in Fig. 11(ii).

4. Routing Algorithms

This section builds dimension-order routing algorithms for the circulants. At the core lies a *routing record generator* for a shortest path from a source to the destination.

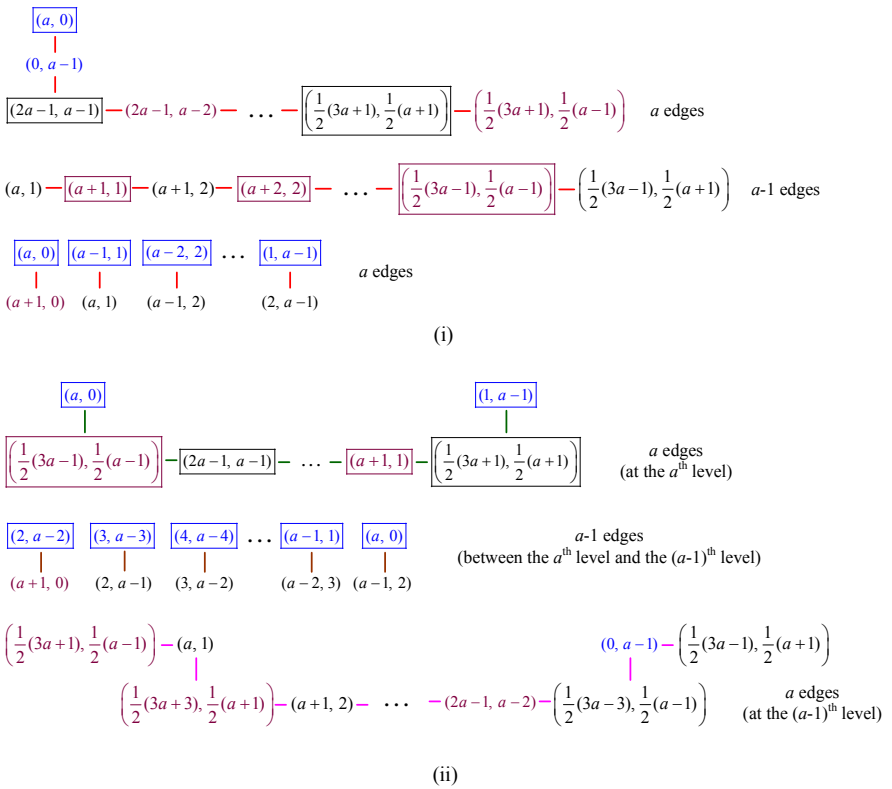

Fig. 11. (i) Incompatible edges in the RTT, and (ii) New edges.

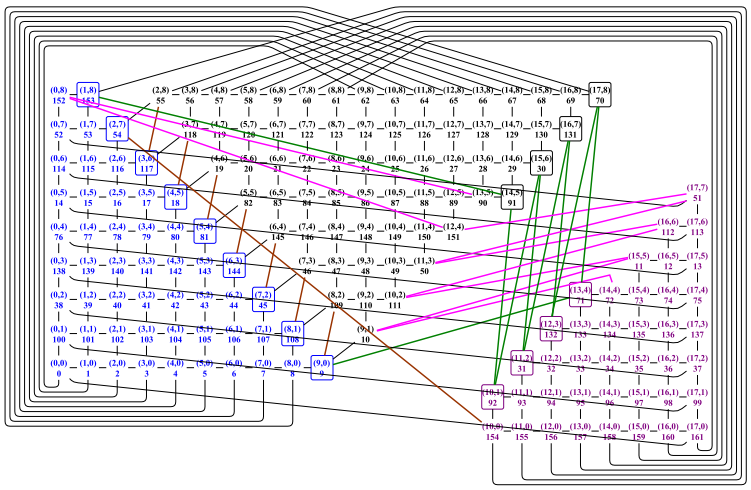

Fig. 12. $\mathcal{C}_{162}(1, 100)$ obtainable from the 18×9 RTT.

The method of attack[7,16] is as follows:

(i) Build a 2D representation of the graph in the Cartesian plane.
(ii) Build a radial layout of the graph relative to a fixed node.
(iii) Construct a plane tessellation in which a "principal tile" exists in juxtaposition with a set of identical tiles. (Vertices in the same relative positions in different tiles represent the same node.) Delineate the span of nodes within a distance of a from all nodes in the principal tile. In the process, find out the least number of tiles for that purpose.
(iv) Obtain the routing record through a computation involving the coordinates of the origins of all tiles in the collection.

4.1. $\mathcal{C}_{2a^2}(1, (a-1)^2)$, $a \equiv 3 \pmod 4$

Let $n = 2a^2$, $s = (a-1)^2$ and $d = 4a - 2$, so $n - s = a^2 + 2a - 1$.

4.1.1. *2D embedding*

Algorithm 1 builds a function ϕ toward an embedding of $\mathcal{C}_{2a^2}(1, (a-1)^2)$ in the 2D plane, and Fig. 13 depicts it while Fig. 14 illustrates it for $a = 15$. Lemma 4.1 shows that the embedding itself is well-defined and correct.

Lemma 4.1.

(i) $\phi(0,0)$, $\phi(0,1)$, $\phi(0,2)$, $\cdots$, $\phi(0, \frac{1}{2}(a-1))$ *are nonnegative and pairwise distinct.*
(ii) $|\phi(0,j) - \phi(0,j-1)| = s$ *or* $n - s$, *where* $1 \le j \le \frac{1}{2}(3a-1)$.
(iii) $\phi(0, j + \frac{1}{2}(a-1)) = 1 + \phi(\frac{1}{2}(3a-3), j)$, $0 \le j \le a$.

Algorithm 1 2D embedding of $\mathcal{C}_{2a^2}(1,(a-1)^2)$

Require: $a \equiv 3 \pmod 4$ and $a \geq 7$

1: $\phi(0,0) = 0$, $\phi(0,1) = (a-1)^2$, $\phi(0,2) = 2(a-1)^2$ // initialization
2: **for** $j = 3$ **to** $\frac{1}{2}(a-1)$ **do**
3: $\quad \phi(0,j) = \phi(0,j-2) - (4a-2)$ // "leftmost lower" column of the L
4: **for** $j = \frac{1}{2}(a+1)$ **to** $\frac{1}{2}(3a-1)$ **do**
5: $\quad \phi(0,j) = \phi(0,j-\frac{1}{2}(a-1)) + \frac{1}{2}(3a-1)$ // "leftmost upper" column
6: **for** $i = 1$ **to** $\frac{1}{2}(3a-3)$ **do**
7: $\quad$ **for** $j = 0$ **to** a **do**
8: $\quad\quad \phi(i,j) = \phi(0,j) + i$ // "lower" segment of the L
9: **for** $i = 1$ **to** $\frac{1}{2}(a-3)$ **do**
10: $\quad$ **for** $j = a+1$ **to** $\frac{1}{2}(3a-1)$ **do**
11: $\quad\quad \phi(i,j) = \phi(0,j) + i$ // "upper" segment of the L

(iv) $\phi(0,j) = 1 + \phi(a-2, a+1+j)$, $0 \leq j \leq \frac{1}{2}(a-3)$.
(v) $\phi(a-1+i,a) = \phi(i,0) + (n-s)$, $0 \leq i \leq \frac{1}{2}(a-1)$.
(vi) $\phi(i, \frac{1}{2}(3a-1)) = \phi(\frac{1}{2}(a+1)+i, 0) + (n-s)$, $0 \leq i \leq a-2$.

Proof. $\phi(0,2), \phi(0,4), \cdots, \phi(0,\frac{1}{2}(a-3))$ are equal to $2s, 2s-d, \cdots, 2s-\frac{1}{4}(a-7)d$, respectively, and $2s-\frac{1}{4}(a-7)d = s+\frac{1}{2}(11a-5)$, i.e., $\phi(0,\frac{1}{2}(a-3)) = s+\frac{1}{2}(11a-5)$. Next, $\phi(0,1), \phi(0,3), \cdots, \phi(0,\frac{1}{2}(a-1))$ are equal to $s, s-d, \cdots, s-\frac{1}{4}(a-3)d$, respectively, and $s = \frac{1}{4}(a-3)d + \frac{1}{2}(3a-1)$, i.e., $\phi(0,\frac{1}{2}(a-1)) = \frac{1}{2}(3a-1)$. It is clear that $\phi(0,2) > \phi(0,4) > \cdots > \phi(0,\frac{1}{2}(a-3)) > \phi(0,1) > \phi(0,3) > \cdots > \phi(0,\frac{1}{2}(a-1)) > \phi(0,0) = 0$.

For (2), $\phi(0,1) = \phi(0,2) - s$, and $\phi(0,3) = \phi(0,2) - (n-s)$, which lead to: $\phi(0,2p-1) = \phi(0,2p) - s$, and $\phi(0,2p+1) = \phi(0,2p) - (n-s)$, where $1 \leq p \leq \frac{1}{4}(a-3)$. Further, $\phi(0,\frac{1}{2}(a+1)) = \phi(0,1) + \frac{1}{2}(3a-1) = s + \frac{1}{2}(3a-1)$ implying

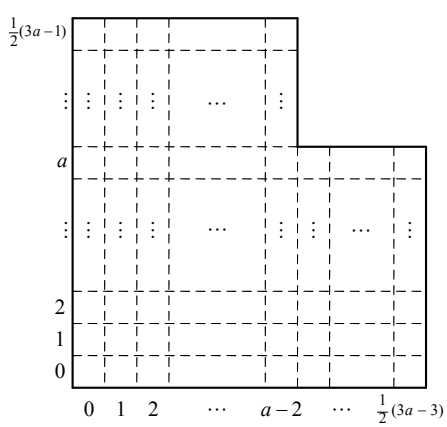

Fig. 13. L-shaped tile of $\mathcal{C}_{2a^2}(1, (a-1)^2)$, $a \equiv 3 \pmod 4$.

$\phi(0, \frac{1}{2}(a+1)) - \phi(0, \frac{1}{2}(a-1)) = s$. These, in turn, lead to: $|\phi(0,j) - \phi(0,j-1)| = s$ or $n-s$, where $1 \le j \le \frac{1}{2}(3a-1)$.

For (3), $\phi(0, j + \frac{1}{2}(a-1)) = \phi(0,j) + \frac{1}{2}(3a-1)$, and $\phi(\frac{1}{2}(3a-3), j) = \phi(0,j) + \frac{1}{2}(3a-3)$.

By Statement (11) of Algorithm 1, $\phi(a-2, a+1+j) = \phi(0, a+1+j) + (a-2)$. Further, by Statement (5), $\phi(0, a+1+j) = \phi(0, j+2) + 2 \times \frac{1}{2}(3a-1)$. Accordingly, $\phi(a-2, a+1+j) = \phi(0, j+2) + (4a-3)$. Finally, by Statement (3), $\phi(0, j+2) = \phi(0,j) - (4a-2)$. Therefore, $\phi(a-2, a+1+j) = \phi(0,j) - 1$.

(5) and (6) are similar. □

The proof of Lemma 4.1 leads to a natural partition of $\{0, \cdots, 2a^2-1\}$ into contiguous sets $A_0, \cdots, A_{\frac{1}{2}(a-3)}$. Whereas A_0 and $A_{\frac{1}{4}(a-3)}$ are of size $3 \times \frac{1}{2}(3a-1) + (a-1) = \frac{1}{2}(11a-5)$ each, the remaining are of size $2 \times \frac{1}{2}(3a-1) + (a-1) = 4a-2$ each. For $a = 15$, they are as follows:

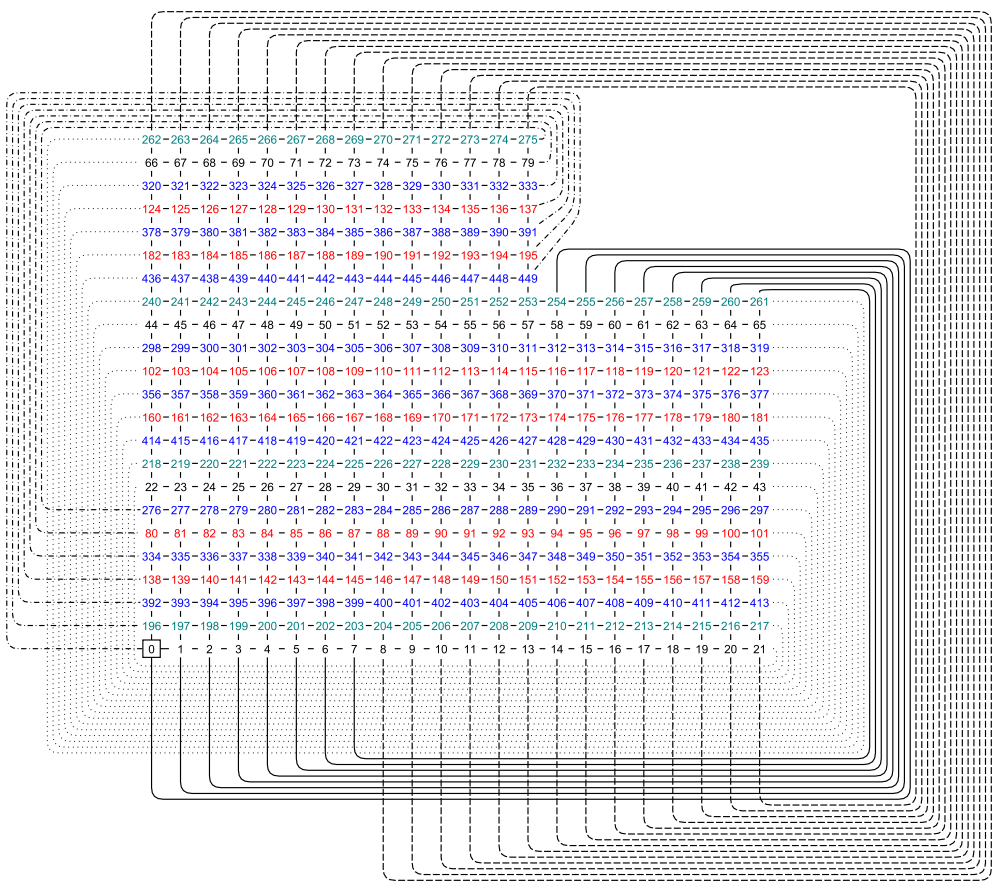

Fig. 14. L-shaped representation of $\mathcal{C}_{450}(1, 196)$.

$$\begin{cases} A_0 = \{0, \cdots, 79\} \text{ spanning rows 0, 7, 14, 21} \end{cases}$$

$$\begin{cases} A_1 = \{80, \cdots, 137\} \text{ spanning rows 5, 12, 19} \\ A_2 = \{138, \cdots, 195\} \text{ spanning rows 3, 10, 17} \end{cases}$$

$$\begin{cases} A_3 = \{196, \cdots, 275\} \text{ spanning rows 1, 8, 15, 22} \end{cases}$$

$$\begin{cases} A_4 = \{276, \cdots, 333\} \text{ spanning rows 6, 13, 20} \\ A_5 = \{334, \cdots, 391\} \text{ spanning rows 4, 11, 18} \\ A_6 = \{392, \cdots, 449\} \text{ spanning rows 2, 9, 16.} \end{cases}$$

4.1.2. *Routing scheme*

Fig. 15(i) presents a plane tessellation while Fig. 15(ii) illustrates it in respect of $a = 7$, and Fig. 16(i) depicts a radial layout of the graph relative to 0. Nodes "inside the diamond" are within a distance of $a - 1$ from 0. There are $2a^2 - 2a + 1$ of them. The remaining are at the periphery, and they are diametrical relative to 0. See Fig. 16(ii) for an example in respect of $a = 7$.

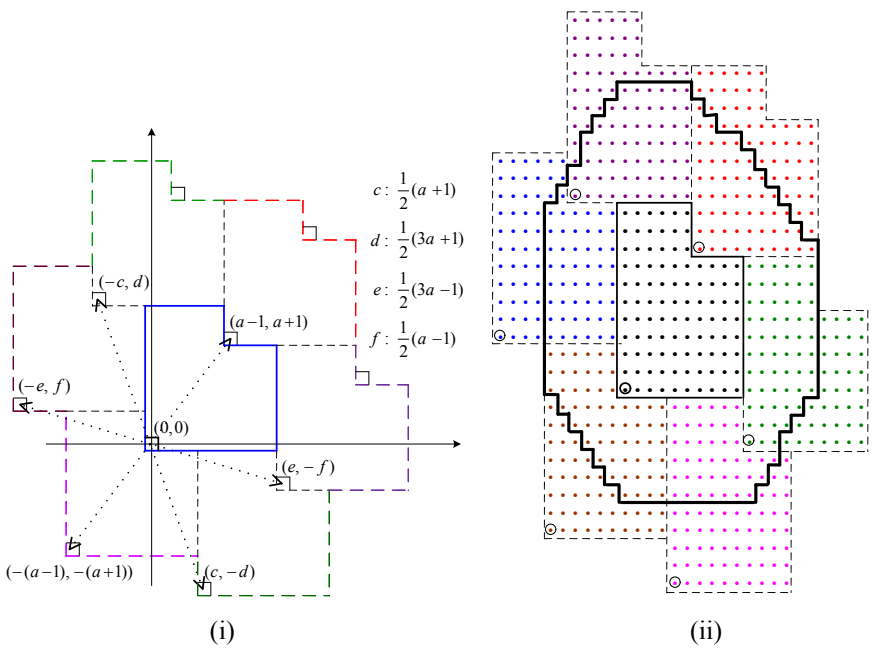

Fig. 15. Plane tessellations using (i) $\mathcal{C}_{2a^2}(1, (a-1)^2)$ and (ii) $\mathcal{C}_{98}(1, 36)$.

The region within the black "zigzag" border in Fig. 15(ii) represents the span of nodes reachable from those in the principal tile (at the center) in a or fewer hops. Note that a total of seven tiles are necessary and sufficient.

Algorithm 2 computes all paths from a source to the destination and returns the routing record. The sign indicates the "E/W" or "N/S" direction.

Algorithm 2 Routing record generator for $\mathcal{C}_{2a^2}(1,(a-1)^2)$

Require: 2D representation of $\mathcal{C}_{2a^2}(1,(a-1)^2)$, $a \equiv 3 \pmod 4$ and $a \geq 7$
input: (s_x, s_y): source node, and (d_x, d_y): destination node
output: $(\Delta x, \Delta y)$: routing record
$\Delta x_0 = d_x - s_x$; $\Delta y_0 = d_y - s_y$;
do in parallel:

$$\begin{aligned}
\Delta x_1 &= \Delta x_0 + (a-1); & \Delta y_1 &= \Delta y_0 + (a+1);\\
\Delta x_2 &= \Delta x_0 - (a-1); & \Delta y_2 &= \Delta y_0 - (a+1);\\
\Delta x_3 &= \Delta x_0 - \tfrac{1}{2}(a+1); & \Delta y_3 &= \Delta y_0 + \tfrac{1}{2}(3a+1);\\
\Delta x_4 &= \Delta x_0 + \tfrac{1}{2}(a+1); & \Delta y_4 &= \Delta y_0 - \tfrac{1}{2}(3a+1);\\
\Delta x_5 &= \Delta x_0 - \tfrac{1}{2}(3a-1); & \Delta y_5 &= \Delta y_0 + \tfrac{1}{2}(a-1);\\
\Delta x_6 &= \Delta x_0 + \tfrac{1}{2}(3a-1); & \Delta y_6 &= \Delta y_0 - \tfrac{1}{2}(a-1);
\end{aligned}$$

return $(\Delta x, \Delta y) := (\Delta x_i, \Delta y_i)$: $|\Delta x_i| + |\Delta y_i|$ is minimum;

4.2. $\mathcal{C}_{2a^2}(1,(a+1)^2)$, $a \equiv 1 \pmod 4$

Let $n = 2a^2$, $s = (a+1)^2$ and $d = 4a+2$. The discussion here is very similar to that in Sec. 4.1, so routine details will be trimmed.

4.2.1. *2D embedding*

Algorithm 3 builds a function ψ toward an embedding of $\mathcal{C}_{2a^2}(1,(a+1)^2)$ in the 2D plane, and Fig. 17 depicts it while Fig. 18 illustrates it for $a = 13$. Lemma 4.2 states that the embedding itself is well-defined and correct.

Lemma 4.2.

(i) $\psi(0,0)$, $\psi(0,1)$, $\psi(0,2)$, $\cdots$, $\psi(0,\frac{1}{2}(a+1))$ *are nonnegative and pairwise distinct.*
(ii) $|\psi(0,j) - \psi(0,j-1)| = s$ *or* $n-s$, *where* $1 \leq j \leq \frac{1}{2}(3a-3)$.

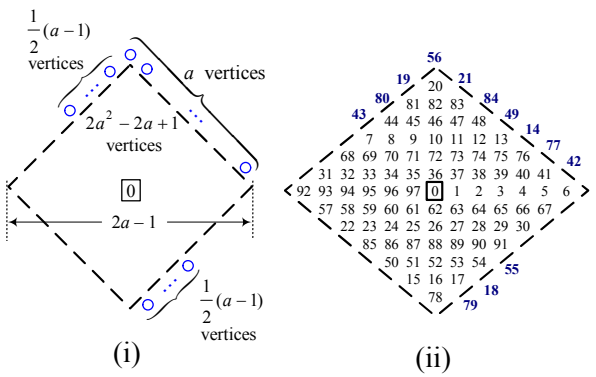

Fig. 16. Radial layouts of (i) $\mathcal{C}_{2a^2}(1,(a-1)^2)$ and (ii) $\mathcal{C}_{98}(1,36)$.

Algorithm 3 2D embedding of $\mathcal{C}_{2a^2}(1,(a+1)^2)$

Require: $a \equiv 1 \pmod 4$ and $a \geq 9$

1: $\psi(0,0) = 0$, $\psi(0,1) = (a+1)^2$, $\psi(0,2) = 4a+2$ // initialization
2: **for** $j = 3$ **to** $\frac{1}{2}(a-1)$ **do**
3: $\quad \psi(0,j) = \psi(0,j-2) + (4a+2)$ // "leftmost lower" column of the L
4: **for** $j = \frac{1}{2}(a+1)$ **to** $\frac{1}{2}(3a-3)$ **do**
5: $\quad \psi(0,j) = \psi(0,j-\frac{1}{2}(a+1)) + \frac{1}{2}(3a+1)$ // "leftmost upper" column
6: **for** $i = 1$ **to** $\frac{1}{2}(3a-1)$ **do**
7: $\quad$ **for** $j = 0$ **to** $a-2$ **do**
8: $\quad\quad \psi(i,j) = \psi(0,j) + i$ // "lower" segment of the L
9: **for** $i = 1$ **to** a **do**
10: $\quad$ **for** $j = a-1$ **to** $\frac{1}{2}(3a-3)$ **do**
11: $\quad\quad \psi(i,j) = \psi(0,j) + i$ // "upper" segment of the L

(iii) $\psi(0, j + \frac{1}{2}(a+1)) = 1 + \psi(\frac{1}{2}(3a-1), j)$, $0 \leq j \leq a-2$.
(iv) $\psi(0,j) = 1 + \psi(a, a-1+j)$, $1 \leq j \leq \frac{1}{2}(a-1)$.
(v) $\psi(a+1+i, a-2) = \psi(i,0) + (n-s)$, $0 \leq i \leq \frac{1}{2}(a-3)$.
(vi) $\psi(i, \frac{1}{2}(3a-3)) = \psi(\frac{1}{2}(a-1)+i, 0) + (n-s)$, $0 \leq i \leq a$.

Proof. Left to the reader. □

There is a partition of $\{0, \cdots, 2a^2-1\}$ into sets $B_0, \cdots, B_{\frac{1}{2}(a-1)}$. While B_0 and $B_{\frac{1}{4}(a-1)}$ are of size $\frac{1}{2}(3a+1) + (a+1) = \frac{1}{2}(5a+3)$ each, the remaining are of size $2 \times \frac{1}{2}(3a+1) + (a+1) = 4a+2$ each. For $a = 13$, the sets follow:

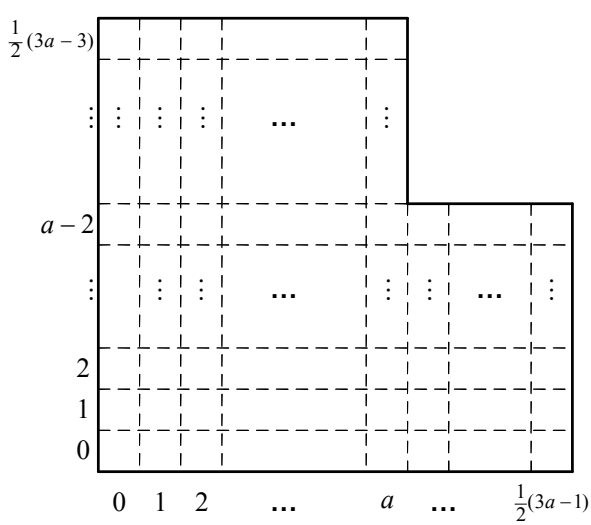

Fig. 17. L-shaped tile of $\mathcal{C}_{2a^2}(1, (a+1)^2)$, $a \equiv 1 \pmod 4$.

$$\begin{cases} B_0 = \{0, \cdots, 53\} \text{ spanning rows 0, 7, 14} \\ B_1 = \{54, \cdots, 107\} \text{ spanning rows 2, 9, 16} \\ B_2 = \{108, \cdots, 161\} \text{ spanning rows 4, 11, 18} \end{cases}$$

$$\{B_3 = \{162, \cdots, 195\} \text{ spanning rows 6, 13}$$

$$\begin{cases} B_4 = \{196, \cdots, 249\} \text{ spanning rows 1, 8, 15} \\ B_5 = \{250, \cdots, 303\} \text{ spanning rows 3, 10, 17} \end{cases}$$

$$\{B_6 = \{304, \cdots, 337\} \text{ spanning rows 5, 12.}$$

4.2.2. *Routing scheme*

Fig. 19(i) presents a plane tessellation while Fig. 19(ii) illustrates it in respect of $a = 9$, and Fig. 20(i) depicts a radial layout of the graph relative to 0. The $2a - 1$ nodes at the periphery are diametrical relative to 0. See Fig. 20(ii) for an example ($a = 9$) and Algorithm 4 for the routing record generator.

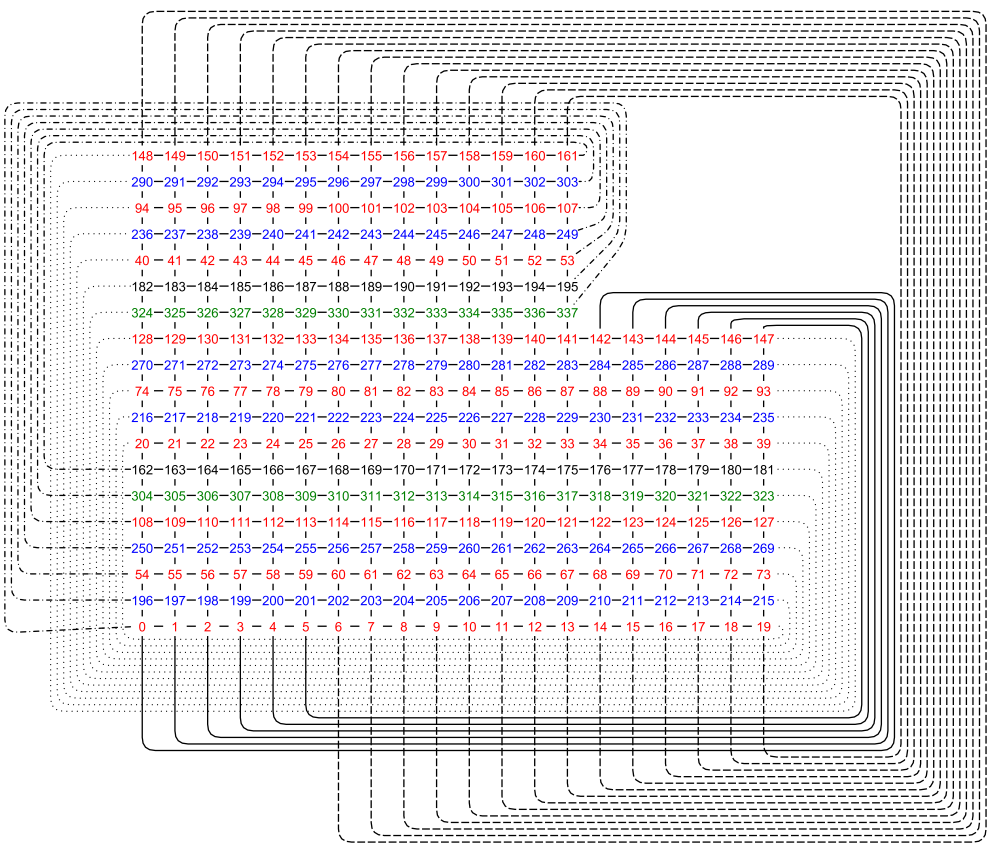

Fig. 18. L-shaped representation of $\mathcal{C}_{338}(1, 196)$.

5. Concluding Remarks

This paper presents a family of four-regular circulants on $2a^2$ vertices, where a is odd. There are two cases: $a \equiv 3 \pmod 4$ and $a \equiv 1 \pmod 4$. The diameter in each case is equal to a that is the theoretical minimum. (A four-regular circulant of diameter a may contain at most $2a^2 + 2a + 1$ vertices, so the graphs are almost dense.)

The circulant in each case is obtainable by trading a total of $3a - 1$ edges of the $2a \times a$ RTT for as many new edges. It turns out that the average distance of each circulant is equal to that of the RTT, viz., $\frac{2}{3}a$ (approx.).[7]

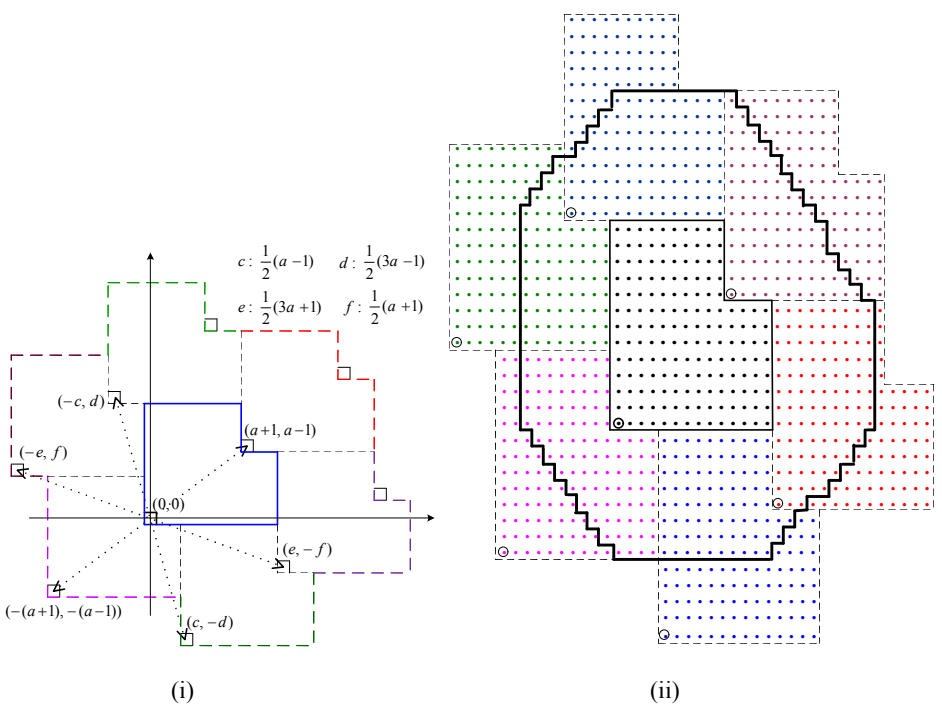

Fig. 19. Plane tessellations using (i) $\mathcal{C}_{2a^2}(1, (a+1)^2)$ and (ii) $\mathcal{C}_{162}(1, 100)$.

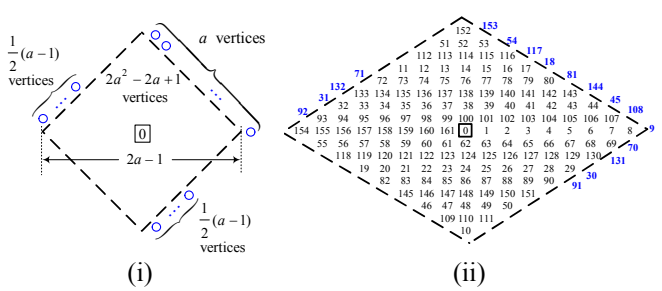

Fig. 20. Radial layouts of (i) $\mathcal{C}_{2a^2}(1, (a+1)^2)$ and (ii) $\mathcal{C}_{162}(1, 100)$.

Algorithm 4 Routing record generator for $\mathcal{C}_{2a^2}(1,(a+1)^2)$

Require: 2D representation of $\mathcal{C}_{2a^2}(1,(a+1)^2)$, $a \equiv 1 \pmod 4$ and $a \geq 9$
input: (s_x, s_y): source node, and (d_x, d_y): destination node
output: $(\Delta x, \Delta y)$: routing record
$\Delta x_0 = d_x - s_x$; $\Delta y_0 = d_y - s_y$;
do in parallel:

$$\begin{aligned}
&\Delta x_1 = \Delta x_0 + (a+1); && \Delta y_1 = \Delta y_0 + (a-1);\\
&\Delta x_2 = \Delta x_0 - (a+1); && \Delta y_2 = \Delta y_0 - (a-1);\\
&\Delta x_3 = \Delta x_0 - \tfrac{1}{2}(a-1); && \Delta y_3 = \Delta y_0 + \tfrac{1}{2}(3a-1);\\
&\Delta x_4 = \Delta x_0 + \tfrac{1}{2}(a-1); && \Delta y_4 = \Delta y_0 - \tfrac{1}{2}(3a-1);\\
&\Delta x_5 = \Delta x_0 - \tfrac{1}{2}(3a+1); && \Delta y_5 = \Delta y_0 + \tfrac{1}{2}(a+1);\\
&\Delta x_6 = \Delta x_0 + \tfrac{1}{2}(3a+1); && \Delta y_6 = \Delta y_0 - \tfrac{1}{2}(a+1);
\end{aligned}$$

return $(\Delta x, \Delta y) := (\Delta x_i, \Delta y_i)$: $|\Delta x_i| + |\Delta y_i|$ is minimum;

The distance-wise vertex layout is such that there are a edges running between vertices at the ath level and as many between vertices at the $(a-1)$th level, contributing to the nonbipartiteness of the graph. Vertices at each lower level being mutually nonadjacent, the odd girth of the graph is equal to $2a - 1 = \sqrt{2n} - 1$, where n is the order of the graph. Meanwhile each circulant is amenable to an efficient dimension-order routing algorithm.

Acknowledgments

Correspondences with Dr. Brian Alspach and Dr. Jonathan D.H. Smith were inspiring. Further, constructive comments from the referees and the Editor-in-chief Dr. Francis Lau were very helpful. The work itself has been partially supported by the St. Cloud State University Researchers Funds.

References

1. B. Alspach and T.D. Parsons, "Isomorphism of circulant graphs and digraphs," *Discrete Math.*, **25** (1979) 97–108.
2. R. Beivide, E. Herrada, J.L. Balcázar and A. Arruabarrena, "Optimal distance networks of low degree for parallel computers," *IEEE Trans. Comput.*, **40**(10) (1991) 1109–1124.
3. J.-C. Bermond, F. Comellas and D.F. Hsu, "Distributed loop computer networks: A survey," *J. Parallel and Distrib. Comp.*, **24** (1995) 2–10.
4. F. Boesch and R. Tindell, "Circulants and their connectivities," *J. Graph Theory*, **8** (1984) 487–499.
5. F. Boesch and J.F. Wang, "Reliable circulant networks with minimum transmission delay," *IEEE Trans. Circuits & Syst.*, **CAS-32**(12) (1985) 1286–1291.
6. J.-Y. Cai, G. Havas, B. Mans, A. Nerurkar, J.-P. Seifert and I. Shparlinski, "On routing in circulant graphs," *Computing and Combinatorics*, LNCS, **1627** (1999) 360–369.
7. J.M. Cámara, M. Moretó, E. Vallejo, R. Beivide, J. Miguel-Alonso, C. Martínez and

J. Navaridas, "Twisted torus topologies for enhanced interconnection networks," *IEEE Trans. Parallel Dist. Syst.*, **21**(12) (2010) 1765–1778.
8. C. Camarero, C. Martínez and R. Beivide, "L-networks: A topological model for regular two-dimensional interconnection networks," *IEEE Trans. Comput.*, In the press.
9. W.L. Dally and B. Towels, *Principles and Practices of Interconnection Networks*. Morgan Kaufman, 2004.
10. T. Dobravec, J. Žerovnik and B. Rovič, "An optimal message routing algorithm for circulant networks," *J. Syst. Arch.*, **52** (2006) 298–306.
11. D.J. Guan, "An optimal message routing algorithm for double-loop networks," *Inf. Process. Lett.*, **65** (1998) 255–260.
12. M.C. Heydemann, "Cayley graphs and interconnection networks," in: *Graph Symmetry* (eds. G. Hahn and G. Sabidussi), Kluwer Acad. Publishing, 1997, pp. 167–224.
13. F.K. Hwang, "A survey on multi-loop networks," *Theoret. Comp. Sci.*, **299** 107–121, 2003.
14. P.K. Jha and R. Prasad, "Hamiltonian decomposition of the rectangular twisted torus," *IEEE Trans. Parallel Dist. Syst.*, **23**(8) (2012) 1504–1507.
15. F.C.M. Lau and G. Chen, "Optimal layouts of midimew networks," *IEEE Trans. Parallel Dist. Syst.*, **7**(9) (1996) 954–961.
16. C. Martínez, E. Vallejo, R. Beivide, C. Izu and, M. Moretó, "Dense Gaussian networks: Suitable topologies for on-chip multiprocessors," *Int. J. Parallel Programming*, **34**(3) (2006) 193–211.
17. S. Nicoloso and U. Pietropaoli, "Isomorphism testing for circulant graphs $\mathcal{C}_n(a, b)$," http://www.optimization-online.org/DB_FILE/2010/03/2577.pdf
18. S.-M. Tang, Y.-L. Wang and C.-Y. Li, "Generalized recursive circulant graphs," *IEEE Trans. Parallel Dist. Syst.* **23**(1) (2012) 87–93.
19. D. Tzvieli, "Minimal diameter double-loop networks-I: Large infinite optimal families," *Networks*, **21** (1991) 387–415.
20. C.K. Wong and D. Coppersmith, "A combinatorial problem related to multimodule memory organization," *J. Assoc. Comput. Macinery*, **21**(3) (1974) 392–402.
21. J. Žerovnik and T. Pisanski, "Computing the diameter in multiple-loop networks," *J. Algorithms*, **14** (1993) 226–243.